JOURNAL OF APPLIED POLYMER SCIENCE VOL. 20, 1231–1244 (1976)

An Analysis of Unsteady One-Dimensional Stretching of a Viscoelastic Fluid

R. Y. TING, *Surface Chemistry Branch, Naval Research Laboratory, Washington, D.C. 20375*

Synopsis

The time-dependent response of a viscoelastic liquid to unsteady one-dimensional stretching deformations was examined. Oldroyd's three-constant model for a viscoelastic fluid was used. Two cases representing two different stretching histories were analyzed: a sine stretching pulse and a step stretching pulse. The results show that high elongational viscosity may be easily reached in both cases. As the relaxation time of the liquid becomes comparable to the pulse width, elongational viscosity increases with the increase in maximum stretching rates. Conditions to maintain high levels of elongational viscosity at a subsequently reduced stretching rate were given as functions of the relaxation time and initial stretching rates. In view of recent turbulent boundary layer data, the results were used to discuss possible explanations of turbulent drag reduction in polymer solutions. It was concluded that the basic mechanisms for drag reduction may be related to the effects of high elongational viscosity and local stabilization of small shear disturbances.

INTRODUCTION

It has been known for some time that dilute solutions of certain high molecular weight polymers exhibit reduced frictional drag in turbulent flow. In explaining the basic mechanisms for drag reduction, it is generally accepted that the viscoelastic effects of polymer solutions are important since drag-reducing polymers do show various viscoelastic properties at high concentrations.[1] However, in spite of the intensive research of the past fifteen years, a completely satisfactory explanation has not yet been found. The reason is quite evident in that the complex nature of the turbulent flow is not understood and yet defies exact mathematical analysis. Furthermore, the viscoelastic properties of dilute polymer solutions are not well known so that the formulation of an exact constitutive law is difficult. The combination of these two limitations makes it necessary to seek an alternative, simplified approach.

There are two distinct features of the turbulent drag reduction phenomenon. The most striking characteristic is probably the fact that the addition of only a few parts per million by weight of polymer can easily cause a reduction of the frictional coefficient by a factor of 2. Secondly, drag reduction is always associated with the presence of wall turbulence, either in turbulent pipe flows or in a turbulent boundary layer. Therefore, one possible approach is to seek for a simple, well-defined flow geometry in which the solution response is substantially different from that in the solvent alone. It is

also preferable that such a flow closely model one of the structural components of a turbulent wall layer, where the drag reduction effect takes place. It is hoped that this type of study may serve as an intermediate step toward the understanding of the mechanisms involved in turbulent drag reduction.

Several investigators have pursued this line of approach, and the results suggest that three flow geometries may be important in formulating explanations for drag reduction: (1) simple transient shear flow, (2) elongational flow, and (3) the stability of small disturbances in steady shear. The various proposed mechanisms are briefly developed here:

1. It was proposed that polymer viscoelasticity affects transient shear flows. Ultman and Denn[2] first suggested that flow structure may be changed if flow velocity exceeds the finite propagation speed of shear waves in a viscoelastic fluid. Ruckenstein[3] later showed that the shear stress in an element of fluid in contact with the wall for a given period of time is smaller in the viscoelastic case than in the Newtonian one. Similar results were also obtained by Hansen.[4] However, in these initial investigations, the convected Maxwell model was employed, where the contribution of the solvent effect was completely neglected. A recent study,[5] using a more complete constitutive relation, reexamined the time-dependent shear flow and showed that viscoelastic effects in this case were negligibly small. The minimal difference between solvent and solution suggests that this flow geometry is not important in turbulent drag reduction.

2. The high viscosity of polymer solutions in elongational flow has been proposed to be responsible for drag reduction. Peterlin,[6] among others, pointed out that polymer molecules may interact with turbulent eddies to locally store energy and change the energy budget by producing a significant viscosity contribution in a dilational flow field. Everage and Gordon[7] carried out a calculation to show the existence of an exceedingly high elongational viscosity in a viscoelastic fluid subjected to a constant steady stretching. Paterson[8] suggested that the high elongational viscosity is related to the dissipation within polymer coil in addition to the work required to perform elastic deformation. And since turbulent drag reduction and elongational viscosity appear to be the only two large macroscopic effects taking place at very low polymer concentrations, it seems to indicate that the two phenomena may be related.

3. The stability of small disturbances in a turbulent boundary layer was also suggested to be involved in the drag reduction effect. Landahl[9] recently applied a two-scale boundary layer turbulence model to examine the effect of polymeric additives on a small scale fluctuating field. His calculation, based on the Batchelor-Hinch suspension model,[10] demonstrated a strong stabilizing effect on high wave number components. Such an effect was expected to lead to an increase in the size of the smallest stress-producing eddies and a corresponding increase in the wall layer thickness. Since the thickened laminar sublayer has been experimentally observed in dilute solutions,[11] it was proposed that the mechanism of drag reduction is associated with the stabilization of secondary disturbances in a turbulent boundary layer.

Since the transient shear response of dilute polymer solutions is very similar to that in water alone,[5] it seems reasonable to rule out the transient shear flow as an important geometry in examining the basic mechanism of turbu-

lent drag reduction. The proposals related to the high elongational viscosity and the stabilization of the secondary disturbances in turbulent boundary layers are attractive, but they also suffer certain limitations. First of all, the elongational viscosity has been shown to be an increasing function of time if a constant, steady stretching is applied.[7] Polymer solutions do not exhibit the high elongational viscosity effect until the stretching rate exceeds certain limiting value and the flow time exceeds the terminal relaxation time of the liquid.[5] Therefore, it may be questionable whether in a turbulent boundary layer conditions would prevail to permit such an effect to take place. Secondly, this proposal was based on the analysis of constant stretching. From practical point of view, the time-dependent material response in the highly transient and chaotic environment of a turbulent boundary layer needs to be examined. The polymer solutions may be reacting to a history of variable stretchings and the solution behavior in this respect is therefore very important in the fundamental understanding of the phenomenon. Lastly, concerning the proposal of the stabilization of local disturbances, Landahl's stability analysis was based on a model which portrays the polymer molecules as long rigid rods, whereas it is well known that the dissolved polymer molecules tend to coil up to maintain a roughly spherical configuration. Hence, the applicability of the stability argument to turbulent drag reduction depends heavily on whether it can be justified to assume a sufficiently extended configuration for these macromolecules. By employing a continuum viscoelastic fluid model, this report represents an initial attempt to try to answer these questions. The response of polymer solutions to some simple stretching deformations will be analyzed, and the results will be used to discuss these proposed drag reduction mechanisms.

MODEL

The Oldroyd three-constant model for a viscoelastic liquid[12] is used,

$$\sigma_{ij} + \lambda_1 \frac{D\sigma_{ij}}{Dt} = 2\eta \left[e_{ij} + \lambda_2 \frac{De_{ij}}{Dt} \right] \tag{1}$$

and the time derivative is defined as

$$\frac{D\sigma_{ij}}{Dt} = \frac{\partial \sigma_{ij}}{\partial t} + v_k \frac{\partial \sigma_{ij}}{\partial x_k} + \omega_{ik}\sigma_{kj} + \omega_{jk}\sigma_{ki} - \sigma_{ik}e_{kj} - \sigma_{jk}e_{ki}$$

where σ_{ij} is the stress tensor, $e_{ij} = (v_{i,j} + v_{j,i})/2$ is the strain-rate tensor, and $\omega_{ij} = (v_{j,i} - v_{i,j})/2$ is the vorticity tensor. This model is qualitatively applicable for the flow of dilute power solutions, because Oldroyd's original formulation was based on a structural model for a colloidal suspension in which Hookean elastic spherical particles were supposed to be distributed in a Newtonian viscous liquid. There are three material constants in eq. (1): η is the viscosity of the liquid, λ_1 is a stress relaxation time, and λ_2 is a strain relaxation time, both having the dimension of time and a positive sign. Oldroyd further explained this model as follows: "The physical model is such that $\lambda_1 > \lambda_2$ and such that, as λ_1 and λ_2 tend to equality, the material becomes more and more exactly a Newtonian liquid of viscosity η." [12] Furthermore, this model was chosen because it has been shown that it may be identified with

the resulting stress–strain relation derived from the equation of motion for isolated polymer molecules based on the dumbbell model.[13] The material constants are related to the molecular properties through the following relationships:

$$\eta = \eta_s(1 + c[\eta]) \tag{2}$$

$$\lambda_2 = \lambda_1/(1 + c[\eta]) \tag{3}$$

where η_s is the viscosity of the solvent, c is the polymer concentration, and $[\eta]$ is the intrinsic viscosity. The time constant λ_1 was identified to be the "terminal relaxation time" λ of polymer solution.[14] By using eqs. (2) and (3), the constitutive relation thus becomes

$$\sigma_{ij} + \lambda\frac{D\sigma_{ij}}{Dt} = 2\eta_s(1 + c[\eta])e_{ij} + 2\eta_s\lambda\frac{De_{ij}}{Dt}. \tag{4}$$

The stress component σ_{ij} can be considered as consisting of the pure-viscous contribution from the solvent, $2\eta_s e_{ij}$, and the contribution of polymers, τ_{ij}. So,

$$\sigma_{ij} = 2\eta_s e_{ij} + \tau_{ij} \tag{5}$$

and it can be shown that τ_{ij} satisfies

$$\tau_{ij} + \lambda\frac{D\tau_{ij}}{Dt} = 2\eta_s c[\eta]e_{ij}. \tag{6}$$

Since only the viscoelastic response is of the interest here, eq. (6) will be used in the following analysis. The viscoelastic stress components τ_{ij} will simply represent the additional contribution the viscoelastic nature of the liquid would introduce besides the Newtonian viscous effect.

ANALYSIS

Now, consider a column of viscoelastic liquid stretched at a rate Γ with its axis oriented in the x_1 -direction. The velocity field

$$[v_i] = \left(\Gamma x, -\frac{\Gamma}{2}y, -\frac{\Gamma}{2}z\right) \tag{7}$$

causes the strain rate tensor to be

$$[e_{ij}] = \begin{bmatrix} \Gamma & 0 & 0 \\ 0 & -\frac{\Gamma}{2} & 0 \\ 0 & 0 & -\frac{\Gamma}{2} \end{bmatrix} \tag{8}$$

and the vorticity tensor $[\omega_{ij}]$ identically zero, so the field is irrotational. The viscoelastic stress components may then be evaluated using eqs. (6) and (8):

$$\tau_{11} + \lambda\left[\frac{\partial\tau_{11}}{\partial t} - 2\Gamma(t)\tau_{11}\right] = 2\eta_s c[\eta]\Gamma(t) \tag{9a}$$

$$\tau_{22} + \lambda\left[\frac{\partial \tau_{22}}{\partial t} + \Gamma(t)\tau_{22}\right] = -\eta_s c[\eta]\Gamma(t) \tag{9b}$$

$$\tau_{33} = \tau_{22}. \tag{9c}$$

All the shear components vanish. Equation (9) can readily be integrated to give

$$\tau_{11}(t) = \frac{2\eta_s c[\eta]}{\lambda} \int_0^t \Gamma(\theta)\left[\exp \int_\theta^t -\frac{1 - 2\lambda\Gamma(s)}{\lambda} ds\right] d\theta \tag{10a}$$

$$\tau_{22}(t) = \frac{-\eta_s c[\eta]}{\lambda} \int_0^t \Gamma(\theta)\left[\exp \int_\theta^t -\frac{1 + \lambda\Gamma(s)}{\lambda} ds\right] d\theta. \tag{10b}$$

These represent the viscoelastic contribution to the total stress tensor in response to a specific stretching history $\Gamma(t)$. Two different cases will now be considered.

Case 1. Sine Stretching Pulse

Recently, Kline et al.[15] and Corino and Brodkey[16] performed flow visualization experiments to observe flow structures near a solid boundary. They reported that turbulence generation was associated with the "bursting" phenomenon taking place in the wall layer region. Fluid elements near the wall were observed to rapidly lift up and "burst" into regions away from the wall. Such bursting processes apparently are of an unsteady stretching nature appearing periodically as pulses in the wall region. Since the detailed time dependence of such stretching motions is not yet known, it is difficult at the present time to assign specific wave forms to such pulses. However, if one can Fourier-analyze such a pulse so to consider it as an ensemble of different sinusoidal modes at discrete frequencies, then it seems to be constructive to examine the viscoelastic response of polymer solutions to a sinusoidal pulse. Assume a stretching history of the form

$$\Gamma(t) = \Gamma_0 \sin \frac{\pi t}{a} \tag{11}$$

where Γ_0 is the peak stretching value and a the pulse width. Substituting into eq. (10), one may obtain expressions for the stress components τ_{11} and τ_{22}. In dimensionless form, for $0 \le t \le a$,

$$\bar{\tau}_{11}(\bar{t}) = \frac{\tau_{11}(t)}{c[\eta]\eta_s\Gamma_0} = \frac{2}{\bar{\lambda}} \exp\left(-\frac{\bar{t}}{\bar{\lambda}} - \frac{2\bar{\Gamma}_0}{\pi} \cos \pi\bar{t}\right) \times \int_0^{\bar{t}} \sin \pi\bar{\theta} \exp\left[\frac{\bar{\theta}}{\bar{\lambda}} + \frac{2\Gamma_0}{\pi} \cos \pi\bar{\theta}\right] d\bar{\theta} \tag{12a}$$

$$\bar{\tau}_{22}(\bar{t}) = \frac{\tau_{22}(t)}{c[\eta]\eta_s\Gamma_0} = \frac{-1}{\bar{\lambda}} \exp\left(-\frac{\bar{t}}{\bar{\lambda}} + \frac{\Gamma_0}{\pi} \cos \pi\bar{t}\right) \times \int_0^{\bar{t}} \sin \pi\bar{\theta} \exp\left[\frac{\bar{\theta}}{\bar{\lambda}} - \frac{\Gamma_0}{\pi} \cos \pi\bar{\theta}\right] d\bar{\theta} \tag{12b}$$

where $\bar{\lambda} = \lambda/a$, $\bar{t} = t/a$, $\bar{\theta} = \theta/a$, and $\bar{\Gamma}_0 = \Gamma_0 a$.

For $t \geq a$ or $\bar{t} \geq 1$, the long time response to the stretching pulse is

$$\bar{\tau}_{11}(\bar{t}) = \frac{2}{\bar{\lambda}} \int_0^1 \sin \pi\bar{\theta} \exp\left[-\frac{\bar{t} - \bar{\theta}}{\bar{\lambda}} + \frac{2\bar{\Gamma}_0}{\pi}(1 + \cos \pi\bar{\theta}) \right] d\bar{\theta} \tag{13a}$$

$$\bar{\tau}_{22}(\bar{t}) = \frac{-1}{\bar{\lambda}} \int_0^1 \sin \pi\bar{\theta} \exp\left[-\frac{\bar{t} - \bar{\theta}}{\bar{\lambda}} - \frac{\Gamma_0}{\pi}(1 + \cos \pi\bar{\theta})\, d\bar{\theta} \right]. \tag{13b}$$

A reduced elongational viscosity is defined as

$$\bar{\eta}(\bar{t}) = \bar{\tau}_{11}(\bar{t}) - \bar{\tau}_{22}(\bar{t}) = \frac{\tau_{11} - \tau_{22}}{c[\eta]\eta_s\Gamma_0}. \tag{14}$$

This definition in dimensionless form allows for the effects of concentration, molecular weight, and solvent viscosity through c, $[\eta]$, and η_s. The time dependence represents the viscoelastic response of the liquid to the deformation, in this case eq. (11), and may be evaluated from eqs. (12) and (13).

Case 2. Step Stretching Pulse

Now, to examine the material behavior responding to a series of variable stretchings, consider the simple case in which a constant stretching rate Γ_0 is applied for a time period of $t = a$. Then, the stretching rate "steps" down to a lower value $p\Gamma_0$, $(p < 1)$, i.e.,

$$\left.\begin{aligned} \Gamma(t) &= \Gamma_0 && 0 < t < a \\ &= p\Gamma_0 \quad (p < 1) && a < t < 2a \\ &= 0 && t > 2a \end{aligned}\right]. \tag{15}$$

By substituting eq. (15) into eq. (10), the stress components may be calculated for each of the three separate time domains. In dimensionless form, they are

(i) $0 < t < a$ or $0 < \bar{t} < 1$:

$$\bar{\tau}_{11}(\bar{t}) = \frac{\tau_{11}(t)}{c[\eta]\eta_s\Gamma_0} = \frac{2}{1 - 2\bar{\lambda}\bar{\Gamma}_0}\left[1 - \exp\left(-\frac{1 - 2\bar{\lambda}\bar{\Gamma}_0}{\bar{\lambda}}\bar{t} \right) \right] \tag{16a}$$

$$\bar{\tau}_{22}(\bar{t}) = \frac{\tau_{22}(t)}{c[\eta]\eta_s\Gamma_0} = \frac{-1}{1 + \bar{\lambda}\bar{\Gamma}_0}\left[1 - \exp\left(-\frac{1 + \bar{\lambda}\bar{\Gamma}_0}{\bar{\lambda}}\bar{t} \right) \right]. \tag{16b}$$

(ii) $a < t < 2a$ or $1 < \bar{t} < 2$:

$$\bar{\tau}_{11}(\bar{t}) = \frac{2}{1 - 2\bar{\lambda}\bar{\Gamma}_0}\left[1 - \exp\left(-\frac{1 - 2\bar{\lambda}\bar{\Gamma}_0}{\bar{\lambda}} \right) \right] \exp\left[-\frac{1 - 2p\bar{\lambda}\bar{\Gamma}_0}{\bar{\lambda}}(\bar{t} - 1) \right] + \frac{2p}{1 - 2p\bar{\lambda}\bar{\Gamma}_0}\left[1 - \exp\left\{ \frac{1 - 2p\bar{\lambda}\bar{\Gamma}_0}{\bar{\lambda}}(\bar{t} - 1) \right\} \right] \tag{17a}$$

$$\bar{\tau}_{22}(\bar{t}) = \frac{-1}{1 + \bar{\lambda}\bar{\Gamma}_0}\left[1 - \exp\left(-\frac{1 + \bar{\lambda}\bar{\Gamma}_0}{\bar{\lambda}} \right) \right] \exp\left[-\frac{1 + p\bar{\lambda}\bar{\Gamma}_0}{\bar{\lambda}}(\bar{t} - 1) \right] - \frac{p}{1 + \bar{\lambda}\bar{\Gamma}_0}\left[1 - \exp\left\{ -\frac{1 + p\bar{\lambda}\bar{\Gamma}_0}{\bar{\lambda}}(\bar{t} - 1) \right\} \right]. \tag{17b}$$

(iii) $t > 2a$ or $\bar{t} > 2$:

$$\bar{\tau}_{11}(\bar{t}) = \frac{2}{1-2\bar{\lambda}\bar{\Gamma}_0}\left[\exp\frac{-\bar{t}+1+2p\bar{\lambda}\bar{\Gamma}_0}{\bar{\lambda}}\right]\left[1-\exp\left(-\frac{1-2\bar{\lambda}\bar{\Gamma}_0}{\bar{\lambda}}\right)\right] + \frac{2p}{1-2p\bar{\lambda}\bar{\Gamma}_0}\exp\left(-\frac{\bar{t}-2}{\bar{\lambda}}\right)\left[1-\exp\left(-\frac{1-2p\bar{\lambda}\bar{\Gamma}_0}{\bar{\lambda}}\right)\right] \quad (18a)$$

$$\bar{\tau}_{22}(\bar{t}) = \frac{-1}{1-2\bar{\lambda}\bar{\Gamma}_0}\exp\left[\frac{-\bar{t}+1-p\bar{\lambda}\bar{\Gamma}_0}{\bar{\lambda}}\right]\left[1-\exp\left(-\frac{1+\bar{\lambda}\bar{\Gamma}_0}{\bar{\lambda}}\right)\right] - \frac{p}{1+p\bar{\lambda}\bar{\Gamma}_0}\exp\left(-\frac{\bar{t}-2}{\bar{\lambda}}\right)\left[1-\exp\left(-\frac{1+p\bar{\lambda}\bar{\Gamma}_0}{\bar{\lambda}}\right)\right]. \quad (18b)$$

The reduced elongational viscosity $\bar{\eta}$, as defined in eq. (14), may now be evaluated. It should be pointed out that in addition to the classical limiting behavior of $\bar{\eta}$ at $\bar{\Gamma}_0 = 1/2\bar{\lambda}$ for stretching, there exists other singularities $\bar{\Gamma}_0 = 1/2p\bar{\lambda}$. However, since $p < 1$, this represents a higher stretching rate; so, from the experimental point of view, it needs not to be concerned with because the first limiting stretching rate will be easier to observe and more interesting.

RESULTS AND DISCUSSION

The response of the viscoelastic liquid to the deformation, eq. (11), is shown in Figure 1. It can be seen that the stress response lags the strain rate input and continues to increase even for $\bar{t} > 0.5$, after the maximum stretching rate Γ_0 is reached at $\bar{t} = 0.5$. For lower Γ_0, $\bar{\eta}$ reaches a peak value slightly before $\bar{t} \to 1$. This maximum gradually shifts to large $\bar{t}$ value for higher and higher $\bar{\Gamma}_0$. Very high elongational viscosity may be reached since the growth of $\bar{\eta}$ becomes more rapid as Γ_0 increases. For $\bar{t} > 1$, the stretching vanishes and an exponential decay of the stresses starts. The decaying rate depends on the relaxation time scale $\bar{\lambda}$; the shorter $\bar{\lambda}$ is the faster the decay becomes. Figure 2 shows the effect of relaxation time $\bar{\lambda}$ on the reduced elongational viscosity $\bar{\eta}$. The values of $\bar{\eta}$ at $\bar{t} = 1$, i.e., the maximum $\bar{\eta}$ in most cases, are plotted against $\bar{\Gamma}_0$ with $\bar{\lambda}$ as a parameter. It again shows that $\bar{\eta}$ increases with $\bar{\Gamma}_0$ very rapidly. Furthermore, the greatest effect seems to take place as $\bar{\lambda} \to 1$. Intuitively, for too small a $\bar{\lambda}$, the material is completely relaxed during the stretching period and behaves more like a Newtonian viscous liquid. For higher $\bar{\lambda}$, the material does not have enough time to allow for the stress buildup. Only as $\bar{\lambda} \sim 0(1)$, the viscoelastic effect is most pronounced.

For a stretching history represented by eq. (15), the growth of elongational viscosity is shown in Figures 3 and 4, respectively, to demonstrate the effects of $\bar{\Gamma}_0$ and $\bar{\lambda}$. The conclusion here is similar to that for the previous case of sine stretching pulse. Namely, at constant $\bar{\lambda}$, the elongational viscosity becomes greater as $\bar{\Gamma}_0$ increases. For fixed $\bar{\Gamma}_0$, the effect is the greatest as $\bar{\lambda} \sim 0(1)$.

The response may generally be described in this way. For $0 < \bar{t} < 1$, $\bar{\eta}$ increases rapidly in response to the first stretching "step" at $\bar{\Gamma} = \bar{\Gamma}_0$. The rate of this increase scales with $\bar{\Gamma}_0$ and $\bar{\lambda}$. For $\bar{t} > 2$, the stretching is completely

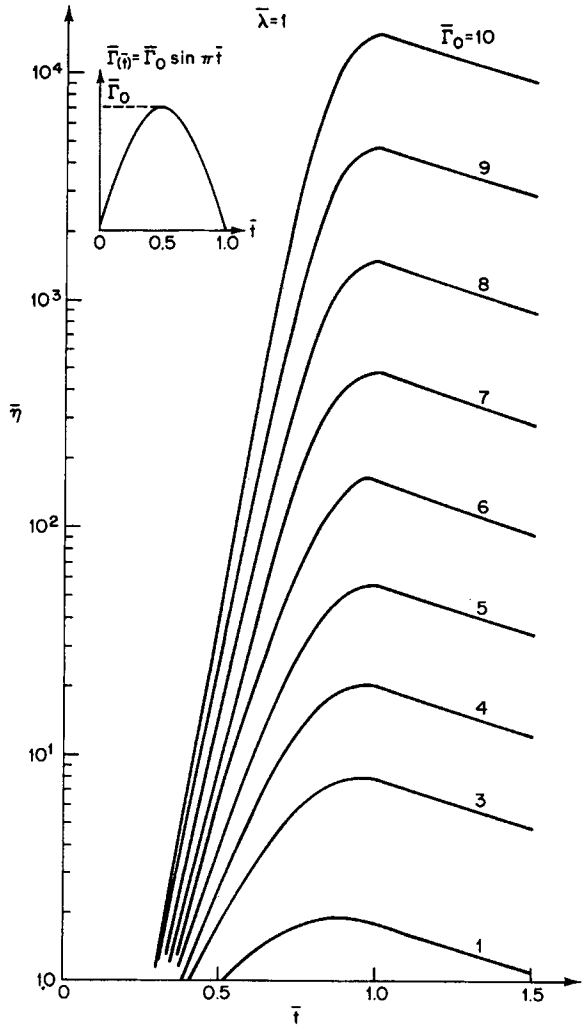

Fig. 1. Growth of elongational viscosity at $\bar{\lambda} = 1$.

cut off, and the stress relaxation takes place in an exponential fashion. The rate of relaxation inversely scales with the relaxation time $\bar{\lambda}$. Note especially the case of $\bar{\lambda} = 0.08$, in which relaxation takes place so rapidly that $\bar{\eta}$ decreases by one decade for a time period $\bar{t}$ of only 0.1. For $1 < \bar{t} < 2$, the liquid experiences a reduction in the stretching rate from $\bar{\Gamma} = \bar{\Gamma}_0$ to $p\bar{\Gamma}_0$ with $p < 1$; the response then depends strongly on the parameter p. For higher p values, the reduced elongational viscosity $\bar{\eta}$ continues to increase from $\bar{t} = 1$, whereas as p decreases, $\bar{\eta}$ may start decreasing. The response is seemingly exponential. Unfortunately, an analytical expression for p for the zero growth of $\bar{\eta}$ could not be obtained.

However, the behavior of maintaining a constant value of $\bar{\eta}$ may be studied numerically for $1 < \bar{t} < 2$ by adjusting the value of p. In Figure 5, this p value for the zero growth of $\bar{\eta}$ is plotted against $\bar{\Gamma}$. For each $\bar{\Gamma}_0$, $\bar{\eta}$ will increase for p values above the curve (represented by $\bar{\eta}\ (\bar{t}) > 0$) and decrease

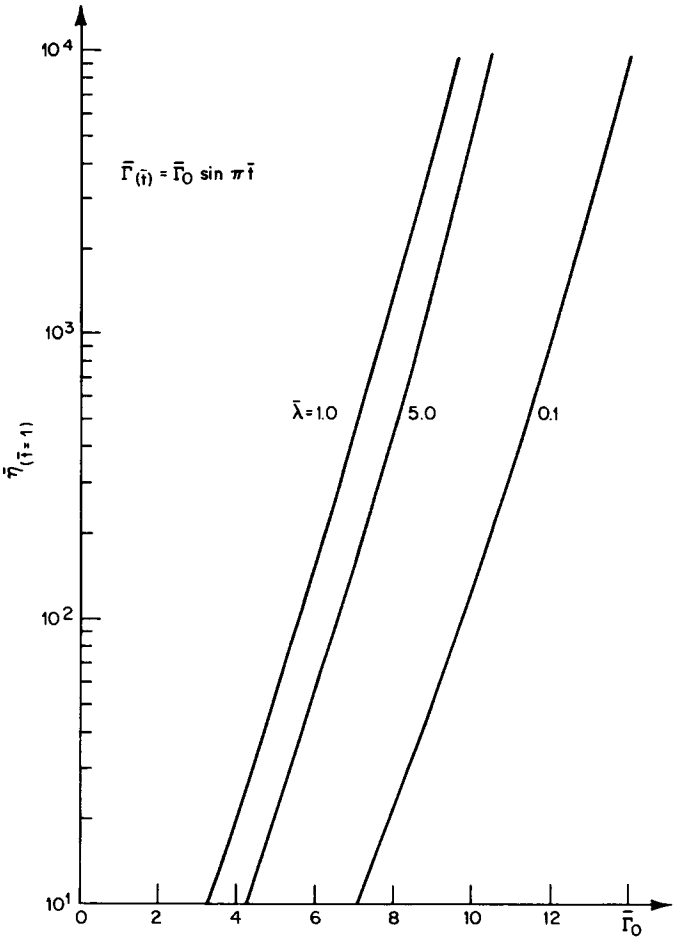

Fig. 2. Elongational viscosity at $\bar{t} = 1$ vs. $\bar{\Gamma}_0$.

for p values below the curve (represented by $\bar{\eta}\ (\bar{t}) < 0$). It is interesting to observe that as $\bar{\Gamma}_0$ or $\bar{\lambda}$ increases, a very small fraction of the original $\bar{\Gamma}_0$ is needed to sustain the growth of $\bar{\eta}$. For example, at $\bar{\lambda} = 1$, $\bar{\Gamma}_0 = 5$, only one tenth of the original stretching is required to maintain $\bar{\eta}$ at the $\bar{\eta}(1)$ level of 1.7×10^3. Hence, a high elongational viscosity may very possibly and easily be reached and maintained in cases where such stretching histories exist.

It is now useful to consider some recent turbulent boundary layer measurements in light of the above calculations. As mentioned above, Kline et al.[15] observed that turbulence generation is associated with the turbulence "bursting" in the wall region. The burst is a violent process occurring primarily in the wall zone in terms of the wall parameter $0 < y + < 100$. The observation suggested a vortex lifting up from the wall region of a turbulent boundary layer like a snapped hair-pin. As it is transported downstream, this vortex is stretched by the main shear, a process described by Corino and Brodkey[16] as the "sweep" of high-speed fluid. The turbulent bursting is highly intermittent and therefore extremely difficult to detect by means of ordinary statistical methods.

More detailed quantitative information is only very recently becoming available through the developments of new experimental techniques. For example, Blackwelder and Kaplan[17] carried out hot-wire measurements of turbulent fluctuations in a turbulent wall layer. Based on selective sampling of

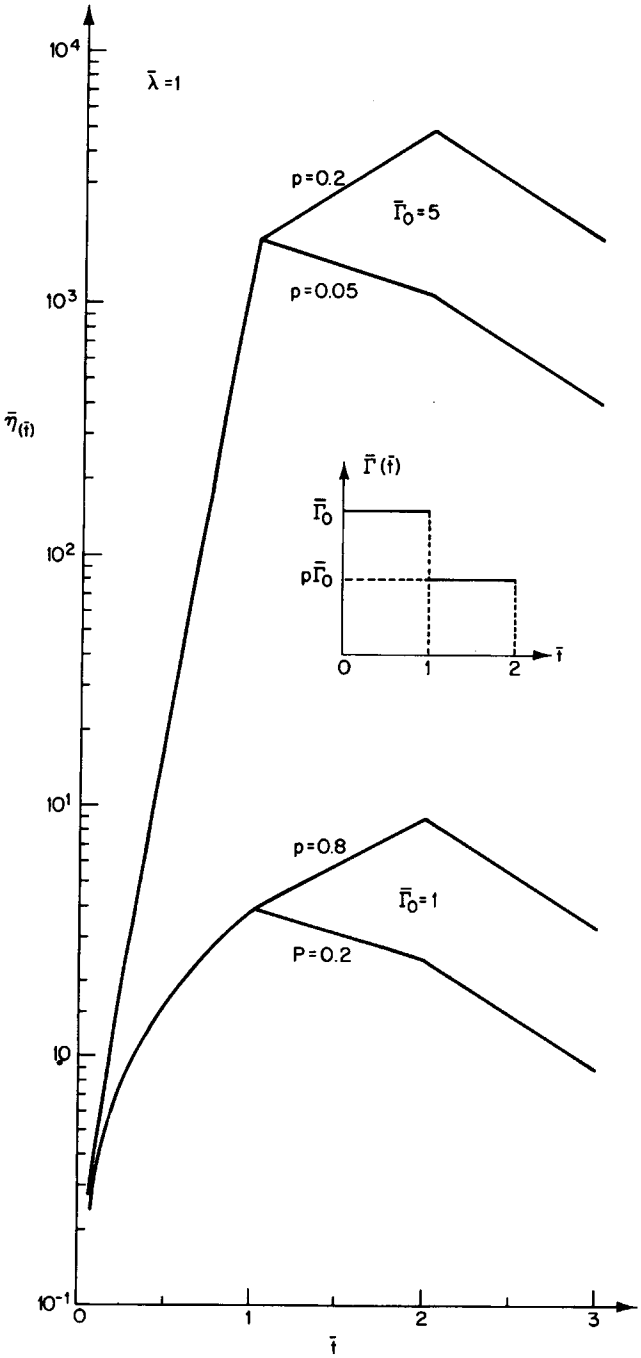

Fig. 3. Viscoelastic response to a step stretching at $\bar{\lambda} = 1$.

signals during bursts, they have succeeded in determining the average instantaneous velocity components just preceding the burst. Figure 6 is one of their typical results, showing the instantaneous streamwise velocity component $u(t)$ at $y^+ = 16.5$ as normalized by the local wall shear velocity u^+ and

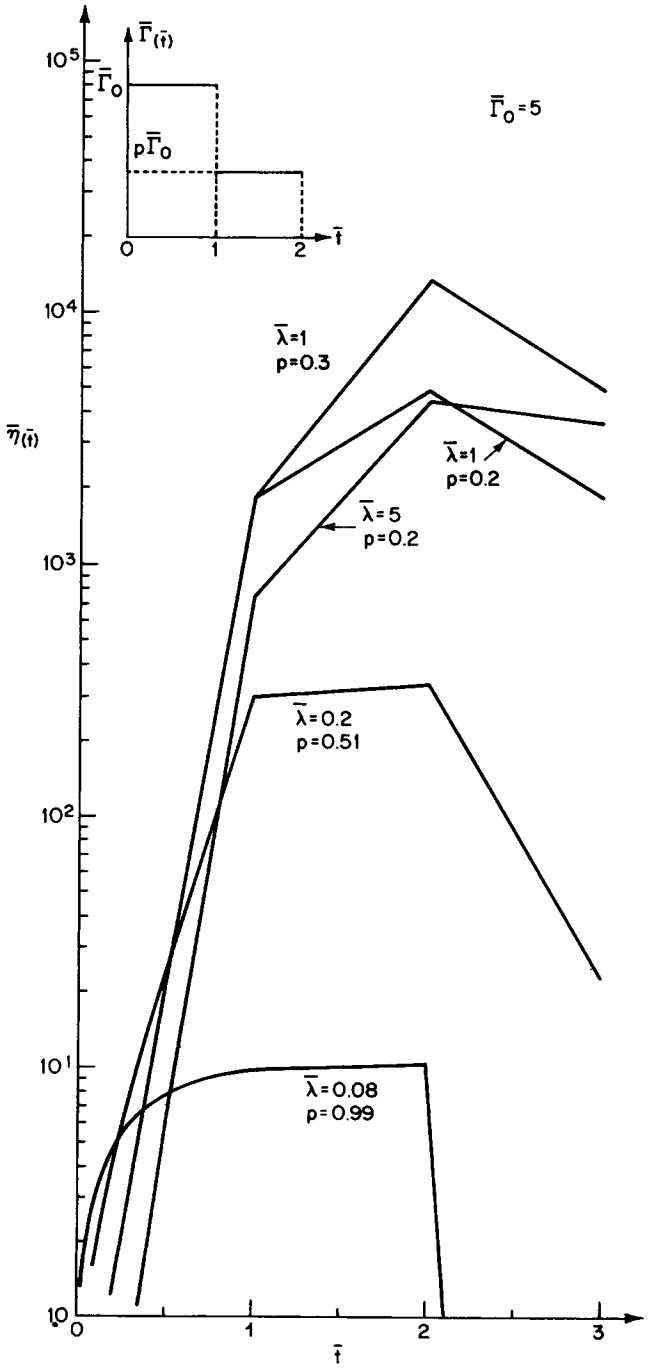

Fig. 4. Viscoelastic response to a step stretching at $\bar{\Gamma}_0 = 5$.

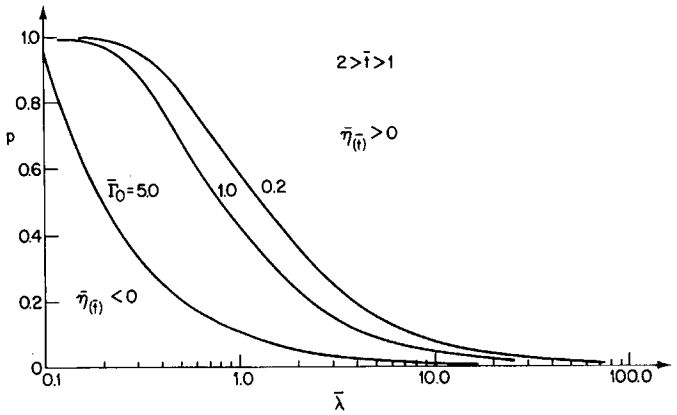

Fig. 5. The values of parameter p for zero growth of $\bar{\eta}$.

the local mean velocity $\bar{u}$. The Reynolds number based on the momentum thickness is 2500. This result clearly shows a large velocity fluctuation about the mean value as the bursting takes place. If one looks at a fluid element from a Lagrangian point of view, it suggests that locally a strong stretching motion is experienced by the fluid. The time scale involved here is of the order of milliseconds.

Now, consider polyethylene oxide, a well-known drag-reducing polymer, for example. A compound with an intrinsic viscosity of 17.6 dl/g in water at 30°C will have an estimated molecular weight 4×10^6 based on the Mark-Houwink equation developed by Bailey et al.[18] The terminal relaxation time as calculated from the molecular theory[14] is 2.27×10^{-3} second. Therefore, if this stretching motion is considered as a stretching pulse, one would have $\bar{\lambda} \sim 0(1)$, in which case the viscoelastic response of the liquid to such motions

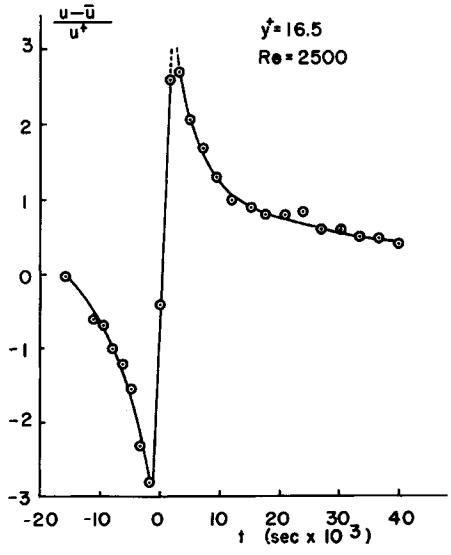

Fig. 6. Instantaneous streamwise velocity in a turbulent boundary layer at $y^+ = 16.5$ (ref. 17).

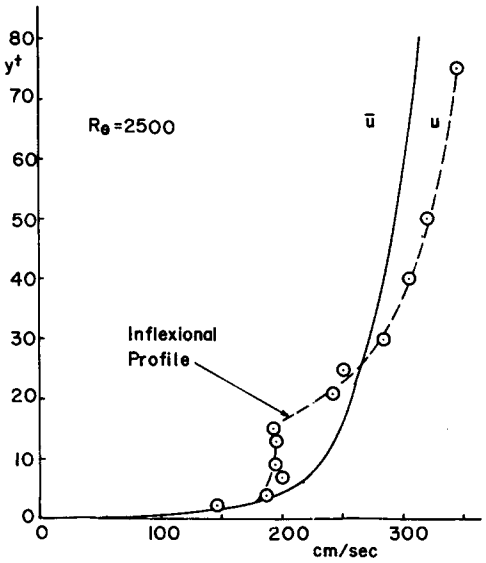

Fig. 7. Instantaneous velocity profile in a turbulent wall layer (ref. 17).

could be the strongest to show very high elongational viscosity. At a reasonable value of $\bar{\lambda} = 10^2$, a 100 parts per million (ppm) dilute aqueous solution of this polymer would exhibit a stress level of $(\tau_{11}-\tau_{22})/\eta_s\Gamma = 17.6$, as opposed to 3 in water,[19] a more than fivefold increase. This produces extensive viscous dissipation in polymer molecules to suppress the "lifting up" of fluid elements that leads to the growth of small eddies which thus results in a substantial reduction in the wall shear stress. The actual stretching rate involved is more difficult to determine at this stage. A detailed Lagrangian analysis of the data, such as those of Blackwelder and Kaplan[17] or of Willmarth and Lu,[20] seems to be in order for future studies. However, from the calculation presented here, it is evident that the effect of high elongational viscosity could be very important in relation to the basic understanding of turbulent drag reduction.

Blackwelder and Kaplan[17] also carried out measurements using a probe containing ten hot wires to obtain an instantaneous velocity profile across the turbulent wall layer. They observed that during bursting there was a substantial streamwise momentum defect followed by an extremely rapid acceleration. While, as mentioned above, the acceleration may suggest a strong stretching of local fluid elements, the streamwise momentum defect suggests a local instability. A reconstruction of their data leads to a plot shown in Figure 7. Compared with the mean velocity profile $\bar{u}(y^+)$, the instantaneous profile $u(y^+)$ exhibits an inflexional character during turbulent bursting. This clearly suggests a strong similarity with the breakdown of the laminar boundary layer flow into turbulence. In fact, Kline et al.[15] in their flow visualization study reported that the observed inflexional instantaneous velocity profiles lead to the growth of an oscillatory disturbance just downstream of the inflexional zone. This growth is rapid and the disturbance reaches a relatively large scale within one or two cycles of oscillation.

Now, if polymer viscoelasticity tends to stabilize this locally unstable flow

condition and thus prevent or suppress the subsequent breakup of fluid elements into large disturbances, this may lead to less turbulence production and therefore reduced turbulent wall shear stress or frictional drag. This was indeed Landahl's argument[9] in relating his stability calculation to this drag reduction mechanism. The second part of the present calculations for the step stretching pulse case clearly shows the favorable conditions under which high elongational viscosity may be maintained at a subsequent lower stretching rate. As indicated in Figure 5, for $\bar{\lambda} = 1$ and $\bar{\Gamma}_0 = 5$, a subsequent stretching rate of $\bar{\Gamma}_0 = 0.5$ can keep a constant level of $\bar{\eta} = 1.7 \times 10^3$, representing a 100-fold increase in the level of tensile stresses in the direction of stretching. According to polymer molecular theory,[21] this may directly cause great molecular extension. It is therefore suggested that the polymer molecules may have very well been largely extended during the bursting process and may lead to the kind of stabilization of small local disturbances presented by Landahl.[9] It is recommended that this possibility of molecular extension in flows such as turbulent shear layers by experimentally verified. Furthermore, for formulating future constitutive relations of viscoelastic liquids applicable under those flow conditions, the possibility that polymers maintain extended configuration should not be neglected.

References

1. J. L. Lumley, *Ann. Rev. Fluid Mech.*, **1,** 367 (1969).
2. J. S. Ultman and M. M. Denn, *Trans. Soc. Rheol.*, **14,** 307 (1970).
3. E. Ruckenstein, *Chem. Eng. Sci.*, **26,** 1075 (1971).
4. R. J. Hansen, *J. Fluid Eng.*, **95,** 23 (1972).
5. R. Y. Ting, J. *Appl. Polym. Sci.*, **16,** 3169 (1972).
6. A. Peterlin, *Nature,* **227,** 598 (1970).
7. A. E. Everage and R. J. Gordon, *A.I.Ch.E.J.*, **17,** 1257 (1971).
8. R. W. Paterson, Ph.D. Dissertation, Harvard University, 1969.
9. M. T. Landahl, Paper presented at the 13th ICTAM Meeting, Moscow, 1972.
10. E. J. Hinch, Ph.D. Thesis, Cambridge University, 1972.
11. C. Elata, J. Lehrer, and A. Kahahovitz, *Isreal J. Tech.*, **4,** 87 (1966).
12. J. G. Oldroyd, *Proc. Roy. Soc. London,* **A200,** 523 (1950).
13. J. L. Lumley, *Phys. Fluid,* **14,** 2282 (1971).
14. B. H. Zimm, *J. Phys. Chem.*, **24,** 269 (1956).
15. S. J. Kline, H. T. Kim, and W. C. Reynolds, *J. Fluid Mech.*, **50,** 133 (1971).
16. E. R. Corino and R. S. Brodkey, *J. Fluid Mech.*, **37,** 1 (1969).
17. R. F. Blackwelder and R. E. Kaplan, in *Turbulent Shear Flow,* AGARD-CP-93, 1972, pp. 5–1.
18. F. E. Bailey, J. C. Kucera, and L. G. Imhof, *J. Polym. Sci.*, **32,** 517 (1958).
19. F. T. Trouton, *Proc. Roy. Soc.*, **A71,** 426 (1906).
20. W. W. Willmarth and S. S. Lu, *J. Fluid Mech.*, **55,** 65 (1972).
21. A. Peterlin, *Pure Appl. Chem.*, **12,** 563 (1966).

Received January 23, 1975
Revised May 1, 1975